Src regulates Golgi structure and KDEL receptor-dependent retrograde transport to the endoplasmic reticulum

F. Bard, L. Mazelin, Christine Péchoux-Longin, V. Malhotra, Pierre Jurdic

HAL Id: hal-02678800

https://hal.inrae.fr/hal-02678800v1

Submitted on 31 May 2020

Src Regulates Golgi Structure and KDEL Receptor-dependent Retrograde Transport to the Endoplasmic Reticulum*

Frédéric Bard‡§, Laetitia Mazelin¶, Christine Péchoux-Longin‖, Vivek Malhotra‡,
and Pierre Jurdic**‡‡**

*From the ‡University of California San Diego Biological Sciences Division, Cell and Developmental Biology Department,
University of California San Diego, La Jolla, CA 92093-0347, the ¶Centre de Génétique Moléculaire et Cellulaire, Unité
Mixte de Recherche 5534 CNRS/Université Claude Bernard, Batiment Grégoire Mendel, 16 Rue Dubois, 69622
Villeurbanne Cedex, France, and the ‖Laboratoire de Génomique et Physiologie de la Lactation, Institut National de la
Recherche Agronomique, Domaine de Vilvert, 78352 Jouy-en-Josas Cedex and the ‡‡Laboratoire de Biologie Moléculaire et
Cellulaire, Unité Mixte de Recherche 5665 CNRS/ENS, Institut National de la Recherche Agronomique 913, Ecole
Normale Supérieure de Lyon, 46, Allée d'Italie, 69007 Lyon, France*

The tyrosine kinase Src is present on the Golgi membranes. Its role, however, in the overall function and organization of the Golgi apparatus is unclear. We have found that in a cell line called SYF, which lacks the three ubiquitous Src-like kinases (Src, Yes, and Fyn), the organization of the Golgi apparatus is perturbed. The Golgi apparatus is composed of collapsed stacks and bloated cisternae in these cells. Expression of an activated form of Src relocated the KDEL receptor (KDEL-R) from the Golgi apparatus to the endoplasmic reticulum. Other Golgi-specific marker proteins were not affected under these conditions. Because of the specific effect of Src on the location of KDEL-R, we tested whether protein transport between ER and the Golgi apparatus involves Src. Transport of *Pseudomonas* exotoxin, which is transported to the ER by binding to the KDEL-R is accelerated by inhibition or genetic ablation of Src. Protein transport from ER to the Golgi apparatus however, is unaffected by Src deletion or inhibition. We propose that Src has an appreciable role in the organization of the Golgi apparatus, which may be linked to its involvement in protein transport from the Golgi apparatus to the endoplasmic reticulum.

Src is activated by various cell surface receptors and phosphorylates numerous cellular proteins (for review, see Refs. 1 and 2). A significant fraction of Src is localized to the perinuclear region and the secretory vesicles in neuronal cells (3, 4). It interacts with and phosphorylates proteins such as dynamin and synapsin (5–7) and synaptophysin (8) or cellugyrin (9), suggesting a role in the regulation of membrane traffic. Src and other Src family tyrosine kinases are also localized to the Golgi apparatus (3, 10). On the Golgi apparatus, Src interacts with the ubiquitin ligase Cbl, and Src activation leads to an increased recruitment of Cbl specifically at the Golgi. This indicates that Src-Cbl signaling might occur at this organelle (10). Further support for this proposal stems from recent findings that show that Src is involved in the activation of Ras on the

Golgi apparatus following mitogenic stimulation (11). Src is also known to phosphorylate and interact with a Golgi apparatus-specific protein, Golgin 67 (12). However, the function of Src signaling at the Golgi remains unknown. The number of signaling molecules that associate with the Golgi membranes and regulate its function and organization is increasing and is known to include protein kinase D, which regulates Golgi-to-plasma membrane trafficking (13) (14), and mitogen-activated protein kinase/extracellular signal-regulated kinase kinase (MEK) and polo-like kinase, which are essential for the fragmentation of the Golgi at the onset of mitosis (15) (16) (17). It is thus reasonable to propose that Src might also be involved in the structural and functional regulation of the Golgi membranes.

A major issue in studies involving Src is the functional redundancy between the Src kinase family, which includes nine members (18). Knock-out studies have revealed that the deletion of Src has relatively mild effects in mice. However, Src knock-out in combination with a deletion of Yes and Fyn, the two other members of the Src family, leads to an early embryonic death (19). A cell line named SYF[1] (for Src, Yes, and Fyn triple knock-out) has been generated from one of these embryos and provides a unique tool to analyze the cellular function of Src.

We found that SYF cells have an aberrant Golgi morphology with compacted stacks and bloated cisternae. Furthermore, expression of an activated form of Src induces the specific exclusion of the KDEL-R from the Golgi apparatus, suggesting an effect on retrograde trafficking. Consistently, the rate of traffic between the Golgi apparatus and the ER of the *Pseudomonas* exotoxin is reduced by Src expression. Deletion of Src does not appear to perturb protein transport in the anterograde pathway from the ER to the plasma membrane via the Golgi apparatus.

EXPERIMENTAL PROCEDURES

Reagents and Cells—The polyclonal Src2 and monoclonal B-12 anti-Src antibodies were purchased from Santa Cruz Biotechnology (Santa Cruz, CA), and the KDEL-R antibody (clone KR-10) was from Calbiochem. Rabbit anti-mannosidase II is a generous gift of Dr. Kelly Morgan

§ To whom correspondence should be addressed. Tel.: 858-534-3752; Fax: 858-534-0555; E-mail: fabard@biomail.ucsd.edu.
** These authors contributed equally to this work.

[1] The abbreviations used are: SYF, Src, Yes, and Fyn triple knock-out; KDEL-R, KDEL receptor; ER, endoplasmic reticulum; PBS, phosphate-buffered saline; PE, *Pseudomonas* exotoxin; VSV, vesicular stomatitis virus; GFP, green fluorescent protein; TGN, trans-Golgi network; F-Golgi, GFP fluorescence in the Golgi area; F-ER, GFP fluorescence in the ER.

Src Regulates Golgi to ER Retrograde Traffic

(University of Georgia). SYF, SYFsrc, and Src+ cells were a kind gift of Drs. Klinghoffer and Soriano (Seattle, WA). Src inhibitor SU6656 was purchased from Calbiochem Novabiochem, and *Pseudomonas* exotoxin came from List Biological Laboratories (Campbell, CA).

Electron Microscopy—Monolayers of SYF and Src+ cells were washed with PBS and fixed *in situ* with 2.5% glutaraldehyde in phosphate buffer, pH 7.4, for 30 min at 4 °C. Cells were then postfixed with 1% osmium tetroxide containing 1.5% potassium cyanoferrate, dehydrated in gradual ethanol (70% to 100%), and embedded in Epon. Thin sections were applied onto 200 mesh copper grids and counterstained with uranyl acetate and lead citrate before examination with a Philips CM 120 transmission electron microscope (CMEABG, Villeurbanne, France).

Pseudomonas Exotoxin Transport Assay—SYF and Src+ cells were grown to near confluence in 24-well plates. 1 h prior to and then during the experiment, cells were incubated in Dulbecco's modified Eagle's medium, without methionine/cysteine, containing 25 mM Hepes. The cells were then incubated with 20 μg/ml *Pseudomonas* exotoxin (PE) or in medium alone (control) for 30 min at 19 °C and then shifted to 37 °C for various periods of time in three wells for PE and three wells of control for each time point. 10 μCi of trans-^{35}S mixture (ICN Pharmaceuticals) was added to each well for 10 min, and the wells were washed twice with PBS before cell lysis and trichloroacetic acid precipitation. After resuspension in sample buffer, the radioactivity in each sample was quantified by scintillation counter, and the average value of treated wells was normalized to the average value of control wells. As an additional control, brefeldin A was added at 5 μg/ml in three wells in the same time as was the PE. For Src drug treatment, Src+ cells were pretreated with 2 μM SU6656 for 30 min prior to the addition of PE.

Vesicular Stomatitis Virus (VSV)-G Protein Transport Assay—GFP-VSV-G protein was transfected using LipofectAMINE® (Invitrogen) according to the manufacturer's recommendation. 24 h after transfection, the cells were transferred at 40 °C for 6 h. Cycloheximide was then added at a concentration of 100 μg/ml. At this stage, which was taken as the 0 min time point, cells were transferred at 32 °C for the indicated period of time before fixation for fluorescence-based analysis.

Immunofluorescence Microscopy—Cells were fixed in 4% formaldehyde in PBS and treated with PBS containing 1% bovine serum albumin and 0.1% Triton X-100 for 1 h before incubation with primary antibodies. Alexa 488- and Alexa 594-conjugated antibodies (Molecular Probes, Eugene, OR) were used as secondary antibodies. Coverslips were mounted with Cytoseal 60 (Richard-Allan Scientific, VWR International) and visualized with a Nikon Microphot-FXA microscope with a Plan-APO 60X objective. Digital images were acquired with an Olympus camera.

Image Analysis and Quantification—The freeware ImageJ 1.29× by Wayne Rasband was used for image quantification and analysis. To quantify the morphology of the Golgi apparatus, the immunofluorescence of mannosidase II was recorded as a digital, 8-bit gray-scale, 1280 × 1024 pixels image. The Golgi labeling image threshold was set at ~90 on a 0–255 black to white scale (all pixels with a value under 90 are excluded from the quantification) to remove background pixels from measurement. A region of interest was defined for each cell, and the perimeter and surface of the Golgi apparatus with a minimum area of three pixels was measured. The dimensionless circularity of the Golgi apparatus was then computed according to the formula $4\pi(\text{sum (areas)}/(\text{sum(perimeters)})^2)$. To quantify the decrease of the KDEL-R immunofluorescence signal at the Golgi in Src-transfected cells, the 8-bit grayscale, non-saturated images of KDEL-R or mannosidase II (as a control) immunofluorescence were set at a threshold value of ~90. For each cell, the number of pixels over threshold and their mean value were measured inside a region of interest covering the perinuclear area. The product of the mean intensity and the number of pixels for each cell was considered the value of immunofluorescence intensity for KDEL-R in the given perinuclear area. Each microscopic field contained one transfected cell and 3–6 control cells, and the average of labeling intensity for the control cell was used to normalize the data. For GFP-VSV-G protein transport assay quantification, we measured the ratio of the average green fluorescence intensity of pixels above background between the Golgi area and the rest of the cell. For each GFP-VSV-G protein green channel image, we used the corresponding GRASP65 (Golgi resident protein) red channel image to generate a "filter," *i.e.* a binary image in which the value of each pixel below background is set to 0, and the value for each pixel above it is set to 1. Each pixel of this binary image was then multiplied by the corresponding pixel (value 0–255) from the green channel image, and the resulting image was then used to measure the average GFP fluorescence above
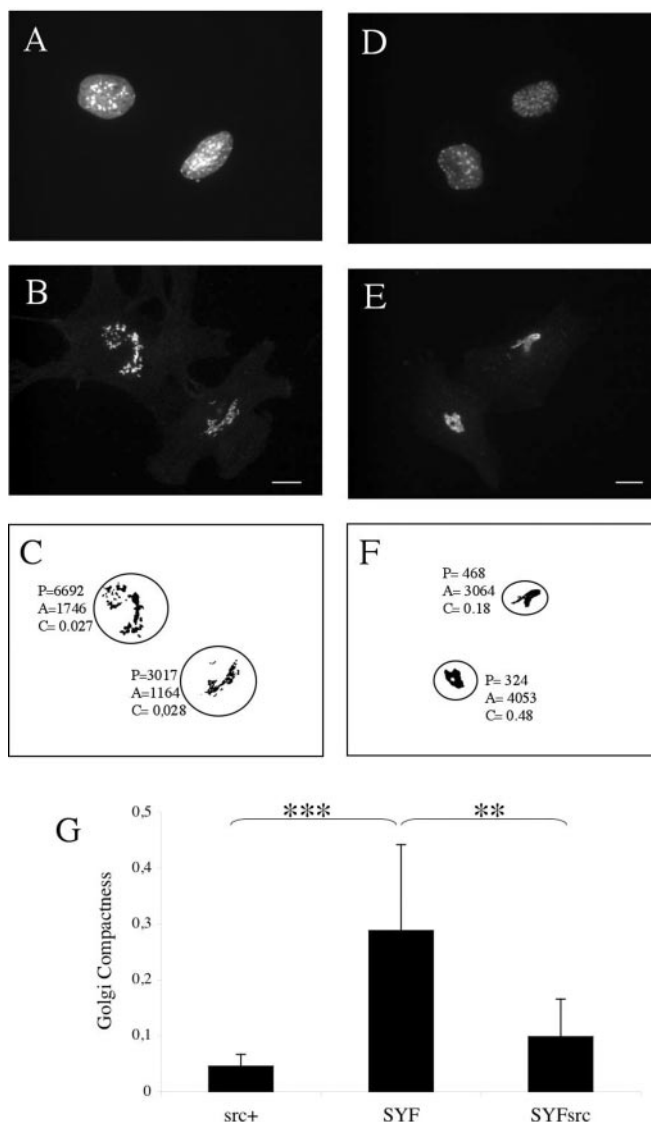

FIG. 1. **SYF cells present a Golgi-compacted morphology.** Src+ (*A*, *B*, and *C*) and SYF (*D*, *E*, and *F*) cells were stained with Hoescht (*A* and *D*) and a polyclonal anti-mannosidase II (*B* and *E*). To quantify the morphology of the Golgi, digital images of mannosidase II labeling were set at a threshold of ~90 (*C* and *F*), excluding all pixels under the threshold intensity value from measurement. The area and the perimeter of each Golgi element of a particular cell were then computed, and their respective sums were used to calculate the compactness of the organelle. The measures for the images in *B* and *E* are shown in *C* and *F* (where *P* is sum of perimeter of Golgi units, *A* is the sum of the areas of Golgi units, and *C* is the compactness value derived from *P* and *A*. See "Experimental Procedures" for details). The compactness values of 22 SYF, 10 Src+, and 9 SYFsrc cells were computed and submitted to statistical analysis (*G*). ***, extremely statistically significant $p < 0.001$; **, very statistically significant $p = 0.0014$. *Bar* is 10 μm in *B* and *F*.

background per pixel in the Golgi area. An inverted image of the filter (0 replaced by 1 and reciprocally) was used to measure the GFP fluorescence above background in the rest of the cell.

Statistical Analysis—For statistical computation and estimation of significance, we used the online software GraphPad® (www.graphpad.com). The circularity of the Golgi apparatus in multiple cells and the normalized results of KDEL-R fluorescence at the Golgi for control and transfected cells were run through unpaired *t* tests. According to GraphPad® recommendations, the computed two-tailed *p* values were considered extremely statistically significant when $p < 0.001$ (noted as *** in Figs. 1*G* and 3*D*), very significant when *p* ranges from 0.001 to 0.01 (noted as ** in Fig. 1*G*), significant when $0.05 > p > 0.01$, and not significant (*n/s* in Fig. 3*H*) when $p > 0.05$.
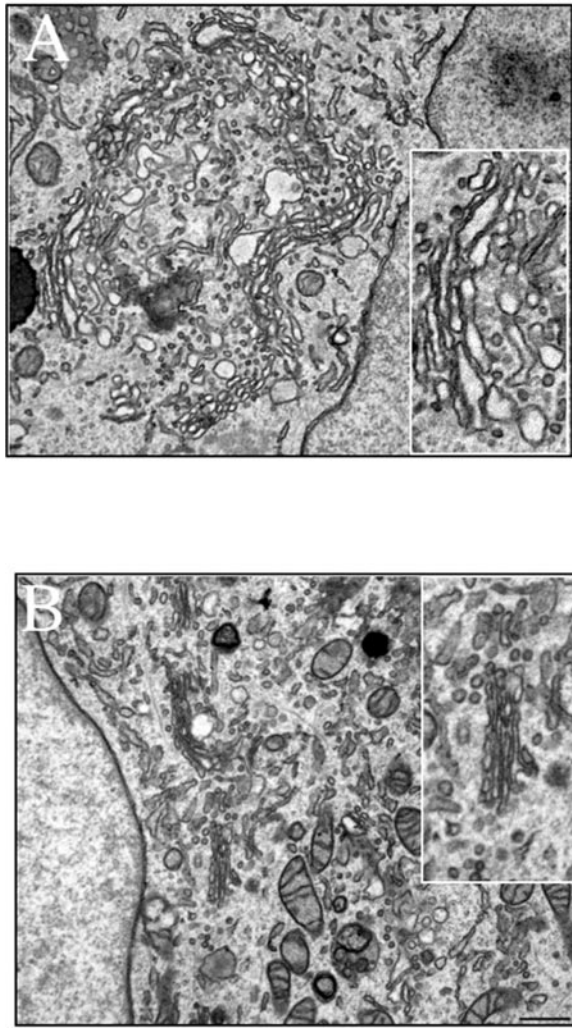
FIG. 2. **The compacted Golgi morphology in SYF cells results from collapsed stacks and bloated cisternae.** SYF (*A*), Src+ (*B*), and SYFsrc (not shown) cells were treated for electron microscopy as described under "Experimental Procedures." 10 cells of each cell line and 4–5 serial sections for each cell, covering most of the Golgi apparatus, were imaged. Representative micrographs of the two different morphologies observed are shown in *panels A* and *B*. *Insets* in *panels A* and *B* are a magnification of the area of the Golgi stacks. *Bar* represents 0.4 μm.

RESULTS

The Golgi Complex Is Compacted in SYF Cells—SYF cells are fibroblasts isolated from triple knock-out embryos for Src, Yes, and Fyn (19). Src+ is a cell line generated from littermate embryos with deletion for Yes and Fyn but with an intact allele for *src*. The cell line called SYFsrc was derived from the SYF cells by stable transfection of a construct expressing c-Src (19). These three cell lines provide useful tools for analyzing the role of Src. To address its role at the Golgi apparatus, we first monitored the morphology of this organelle in SYF cells by immunostaining with an antibody for mannosidase II, which is localized primarily to the medial Golgi cisternae. The Golgi apparatus in mammalian cells is composed of 40–80 stacks that are connected to each other and concentrated in the perinuclear region. In Src+ cells (Fig 1*B*), the Golgi apparatus was relatively normal as compared with control cells like NIH3T3. In contrast, a large proportion of SYF cells displayed an unusually compact Golgi morphology (Fig. 1*E*). To evaluate the overall structure of the Golgi, we developed a statistical test based on the epifluorescence images of the Golgi apparatus. A confocal based three-dimensional reconstruction of the
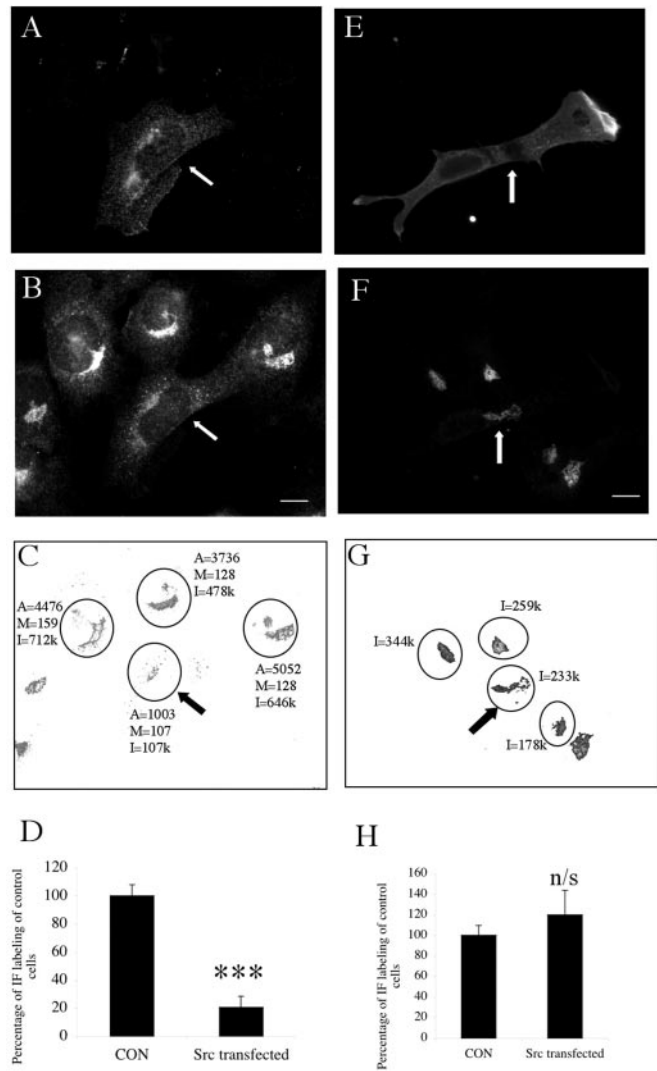

FIG. 3. **The KDEL-R is redistributed following SrcE378G transfection.** SYF cells were transfected with a SrcE378G expression plasmid, fixed 12 h later, and labeled with the anti-Src polyclonal antibody Src2 (*A*) and the anti KDEL-R monoclonal antibody (*B*) or the monoclonal anti phosphotyrosine PY99 (*E*) and the polyclonal anti-mannosidase II (*F*). To quantify the fluorescence at the Golgi, the digital images were set at a threshold of ~90 (C and G), and the total number of pixels above threshold, their mean intensity, and the fluorescent intensity in the perinuclear area (*circles*) of each cell were computed. In *panels C* and *G*, the particular measurements for the images *B* and *F*, respectively, are shown (*A* denotes the number of pixels, *M* is the mean value of intensity, and *I* is fluorescent intensity, the product of *A* and *M*). Each intensity value was then normalized to the mean intensity of control cells (*CON*) in the same image to allow statistical analysis (*D* and *H*); 27 control cells and 7 transfected cells were analyzed for KDEL-R, and 28 control cells and 10 transfected cells were analyzed for mannosidase II. *Arrows* point to transfected cells. ***, extremely statistically significant; *n/s*, not statistically significant. *Bar* in *panels B* and *F* is 10 μm.

Golgi showed that the organelle is relatively flat in SYF, SYFsrc, and Src+ cell lines in culture (data not shown); therefore a morphological analysis in the two dimensions of an epifluorescence image gives a good approximation of the three-dimensional structure of the Golgi. A dispersed, elongated morphology represents a longer perimeter (the enveloping surface in three dimensions) compared with a compact morphology for the same area (the volume in three dimensions). By factoring in the area of a structure with the square value of its perimeter and multiplying it by 4π, one obtains a dimensionless number called circularity (equal to one for a perfect circle). Because the Golgi apparatus is generally formed of several clusters of Golgi

FIG. 4. **Src expression reduces the rate of Golgi to ER traffic of the *Pseudomonas* exotoxin.** *A*, SYF, SYF-src, and SYFsrc+ cells treated with SU6656 for 30 min were incubated at 19 °C for 30 min with 20 ng/ml PE before transfer at 37 °C for 15, 30, 60, 90, or 120 min. For each time point, three identical wells of cells were subjected to a 10-min pulse labeling with [^{35}S]methionine. Protein synthesis activity was then measured by scintillation and averaged before normalization to the synthesis in control cells. Control cells were treated identically except for the addition of the toxin. A control including a treatment with brefeldin A at the same time as the toxin shows that the effect of the toxin is dependent on retrograde traffic through the Golgi apparatus. The results shown are representative of three independent experiments. *Error bars* represent the standard deviation between the three wells. *B*, to test whether Src expression regulates endocytosis and traffic from endosomes to the Golgi of the exotoxin, PE traffic was followed by microscopy. PE was first covalently labeled with the Alexa 594 fluorophore. The cells were incubated with this fluorescent toxin at 19 °C for 30 min and then fixed (*two upper*) or shifted for 15′, 30′, 45′, and 60′ (*two lower rows*) at 37 °C before fixation. The cells were then labeled and imaged for mannosidase II (*MannII*) and the Alexa-594-labeled toxin (*PE594*).
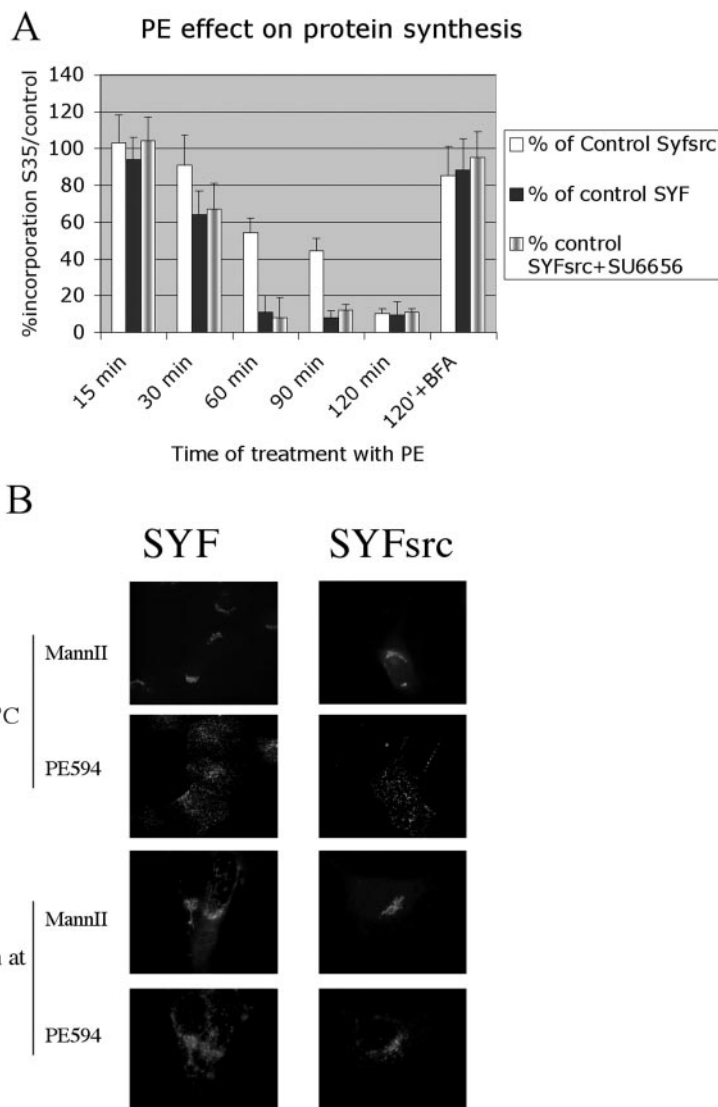
stacks, we used the same formula but with the sum of the areas of the clusters and the sum of their perimeters to calculate the "compactness" of the whole structure. Therefore, the compactness parameter computes both the fragmentation of the Golgi (a Golgi composed of two perfectly circular clusters will have a value of 0.5, with the circularity of each cluster giving a parameter independent of size). Using this method, we found that SYF cells have a statistically significant, more compact Golgi apparatus than either Src+ cells (SYF compactness is equal to 0.288 on average *versus* 0.046 for Src+ cells; $p < 0.0001$) (Fig. 1*G*) or SYFsrc cells (compactness for SYFsrc is 0.099; $p = 0.0014$). The Golgi apparatus of SYFsrc cells was slightly more compact on average than Src+ cells, which is somewhat surprising because by Western blot we found that SYFsrc cells, by comparison with Src+, express higher levels of Src protein (data not shown). However, this could be explained by the high variability of Src expression levels in SYFsrc that we observed by immunofluorescence (data not shown) and by the more heterogeneous Golgi morphology in this cell line as reflected in the higher standard deviation of compactness among cells (Fig. 1*G*). We thus conclude that expression or deletion of Src perturbs the Golgi morphology. Other intracellular structures, such as the focal adhesion system, actin cytoskeleton, and the microtubule network, are not significantly different in SYF

compared with control cells (19).[2]

To further analyze the organization of collapsed Golgi apparatus, Src+, SYFsrc, and SYF cells were imaged by electron microscopy. ~10 cells for each cell line and 4–5 serial sections for each cell were imaged; the most representative photographs are shown in Fig. 2. In SYF cells, the Golgi apparatus was collapsed into a compact structure in which the individual stacks could not be identified (Fig. 2*A*). Interestingly, the individual Golgi cisternae were enlarged in SYF cells (Fig. 2*A*, *inset*) compared with their Src+ counterparts (Fig. 2*B*, *inset*). In Src+ (Fig. 2*B*) and SYFsrc cells (not shown), stacks appeared normal. This overall Golgi organization in SYF cells compares well with the organization of the Golgi apparatus observed at the immunofluorescence level.

Src Activation Leads to the Dispersion of the KDEL Receptor from the Golgi—The effect of Src on the Golgi apparatus organization and our previous findings that Src regulates the amount of Cbl associated with the Golgi membranes (10) prompted us to test whether Src affects the distribution of Golgi-specific proteins. KDEL-R mediates recycling of ER resident proteins that have escaped to the Golgi apparatus by binding to their KDEL sequence. Although the steady state distribution of this receptor is mostly at the Golgi apparatus, it

---

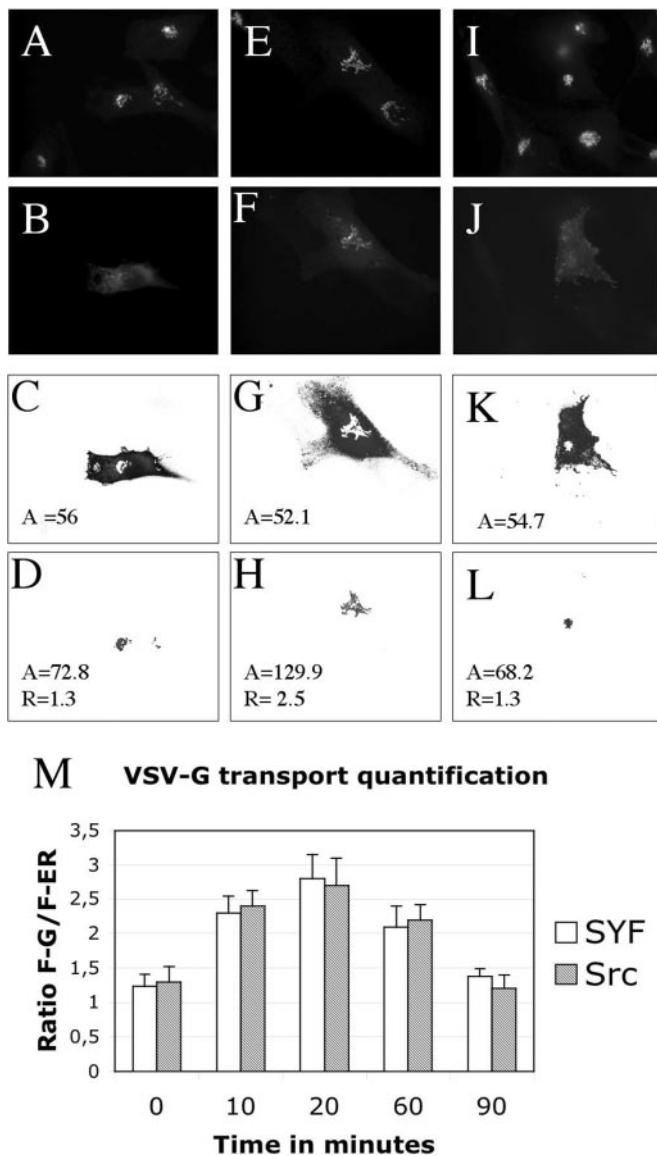[2] F. Bard and P. Jurdic, unpublished observations.

FIG. 5. **The deletion of Src does not affect transport of VSV-G protein in the anterograde pathway.** Src+ and SYF cells were transfected with GFP-VSVGtsO45. After 24 h, the cells were shifted to 40 °C for 6 h, then cycloheximide was added to the culture medium at 100 μg/ml. Cells were then either fixed (time 0) or shifted to 32 °C for various times up to 90 min. Representative example of cells at 0 min (*A*, *B*, *C*, and *D*), 20 min (*E*, *F*, *G*, and *H*), and 90 min (*I*, *J*, *K*, and *L*) are shown. The cells were labeled with the rabbit polyclonal anti-GRASP 65 to visualize the Golgi (*A*, *E*, and *I*) and imaged for GFP (*B*, *F*, and *J*). The images of the GFP image were used as filters to select, from the GFP image with fluorescence above background, the pixels that were not present in the Golgi region (*C*, *G*, and *K*) and the pixels that were present in the Golgi region (D, H, L). The average intensity (*A*, in *panels C*, *D*, *G*, *H*, *K*, and *L*) and the ratio (*R*, in *panels D*, *H*, and *L*) of the fluorescence at the Golgi and in the rest of the cell were then measured. 25 cells for each cell line and for each time point (0, 10, 20, 60, and 90 min) were analyzed, and the results (*M*) were submitted to statistical analysis; although a statistically significant difference was found between different time points, no difference could be detected between cell lines at a same time point.

cycles continuously between the Golgi membranes and ER, and a modification of its distribution reflects an alteration in its trafficking rate (20). We found that KDEL-R was displaced from the Golgi into a dispersed, punctate pattern following expression of an activated form of Src, SrcE378G, in SYF and NIH3T3 cells (Fig. 3, *A–C*, and data not shown). To quantify this effect, we measured the total specific fluorescence signal at the Golgi apparatus (see "Experimental Procedures") for each

cell in a given field, typically containing 1–2 transfected cells and 3–6 non-transfected cells. We then normalized the results by expressing the fluorescence signal as a percentage of the mean of control cells in the same image. Therefore, different images and different experiments can be compared, as this quantification is independent of variations in camera settings and immunofluorescence conditions. We found that KDEL-R immunofluorescence at the Golgi was reduced to 20.6% in average value compared with control cells (Fig. 3*C*). In contrast, using the same method, we found that mannosidase II labeling was not affected in SrcE378G transfected cells (119% of the mean intensity in control cells) (Fig. 3*F*). Other Golgi markers, including the lectin wheat germ agglutinin, peripheral proteins such as giantin, GRASP65, GRASP55, and GM130 (data not shown) as well as a Golgi enzyme such as the β 1,4-galactosyl-transferase 1 (data not shown) were not, at the visual level, affected by the expression of activated Src.

Src Expression Reduces the Rate of Golgi-to-ER Traffic of the Pseudomonas Exotoxin—The effect of Src on KDEL-R distribution suggests that Src may be involved in retrograde traffic from the Golgi apparatus to the ER. We used the bacterial PE, which is transported after endocytosis to the ER via the Golgi apparatus (21). PE binds to KDEL-R by its KDEL-like sequence that insures its transport to the ER. Upon reaching the ER, it is translocated to the cytosol and inhibits protein synthesis (22). To test the kinetics of transport of PE, we measured the delay between PE internalization and the onset of protein synthesis inhibition induced by PE. SYF, SYFsrc, or SYFsrc cells, treated with 2 μM of the Src inhibitor SU6656 (23), were first incubated with 20 ng/ml PE at 19 °C for 1 h. This allows for efficient binding of PE and its accumulation in the endosomal compartment. The cells were then shifted to 37 °C for various periods of time before a 10-min pulse of cysteine S35, which was immediately followed by cell lysis. Proteins in cell lysates were precipitated, and radioactivity was counted by scintillation. The reference level was measured with control cells treated identically except for the addition of PE. As a control, we checked that the effect on protein synthesis is dependent on an intact Golgi apparatus. This was carried out by treating the cells, in addition to PE, with the drug brefeldin A, which fuses the Golgi apparatus with the ER, therefore inhibiting retrograde transport. Treatment with brefeldin A inhibited the PE-mediated effects on protein synthesis (Fig 4*A*). To test whether Src expression perturbs the traffic of PE, the cell lines SYF and SYFsrc were compared. Maximal protein synthesis inhibition by PE was obtained after 60 min in SYF cells (Fig 4*A*). In SYFsrc cells, it took twice as long to reach a similar effect on protein synthesis (Fig 4*A*), indicating that, in the presence of Src, PE traffic to the ER is slower. Consistently, treatment of SYFsrc cells with the Src inhibitor SU6656, prior to addition of PE, reduced the kinetic of PE effect to a level similar to SYF cells (Fig 4*A*), indicating that Src-mediated effect on PE transport is direct. To address the possibility that this regulation could occur at the level of endocytosis or endosomal sorting, we followed the intracellular traffic of PE. We labeled PE by covalent attachment of the fluorescent dye Alexa 594® (P3-A594). SYF, Src+, and SYFsrc cells were incubated with PE-A594 at 19 °C for 30 min and then transferred to 37 °C. At 19 °C, PE-A594 accumulated in the endosomes and did not colocalize with the Golgi marker mannosidase II (Fig. 4*B*). However, after 45 min of incubation at 37 °C, PE began accumulating in the TGN/Golgi compartment in both SYF and SYFsrc, reaching maximum accumulation after 60 min. The amount of PE-A594 that was accumulated in the TGN/Golgi was appreciably lower than the amount detected in the endosomes, suggesting that a significant fraction was degraded in

Src Regulates Golgi to ER Retrograde Traffic

lysosomes. Nevertheless, the kinetics of accumulation of PE-594 in the TGN/Golgi was not significantly different in SYF, Src+, or SYFsrc, indicating that Src does not affect endocytosis or transport of PE from the endosomes to the TGN/Golgi apparatus.

Src Is Not Involved in Transport of VSV-G Protein along the Secretory Pathway—We used the tsO45VSV-G protein as a marker for the trafficking along the secretory pathway. At 40 °C, the tsO45VSV-G protein is retained in the ER because of a folding defect. Upon shifting to 32 °C, the tsO45VSV-G protein folds correctly and exits ER in a synchronous wave as described previously (24). SYF, SYFsrc, and Src+ cells were transfected with a GFP-tsO45VSV-G protein-expressing plasmid and incubated at 40 °C for 6 h to allow accumulation in the ER. The cells were then shifted to 32 °C for various times. Cells were labeled for GRASP65, a Golgi-associated protein, and DNA. In all cell lines tested, VSV-G protein accumulated in the Golgi at the same rate and exited the Golgi apparatus with similar kinetics. To measure more precisely the kinetics of VSV-G protein transport, we devised a quantification scheme based on the ratio of the average GFP fluorescence in the Golgi area (F-Golgi) over the average GFP fluorescence in the rest of the cell (F-ER). Only the fluorescence above background was computed using a threshold value set above the fluorescence of neighboring, untransfected cells (see Fig. 5, *C*, *G*, or *K*, for examples of threshold setting). To measure F-Golgi and F-ER, we used filters generated from the corresponding Golgi-labeling, GRASP65 image (see Fig. 5, *D*, *H*, or *L*, for examples of the resulting images). By using this procedure, we found that the ratio of F-Golgi/F-ER is close to 1 when the cells are kept at 40 °C and the VSV-G protein is localized in the ER. This is due to the fact that the Golgi apparatus is at the center of the cell and surrounded by ER membranes. The ER membranes are spread throughout the cell, which lowers the average value of fluorescence per pixel. The area of the Golgi apparatus therefore is at an equivalent level of fluorescence as the ER. 20 min after switching to 32 °C, the GFP-VSV-G protein accumulated significantly in the Golgi area, and the ratio F-Golgi/F-ER peaked between 2.5 and 3. The difference of ratio between 0 and 20 min in one cell line was considered very statistically significant ($p = 0.005$), indicating that our method of quantification is relatively sensitive. The ratio then slowly decreases and again reaches a value close to 1 after 90 min, a time at which most of the VSV-G protein has exited the Golgi apparatus. No statistically significant difference in the kinetics of transport of VSV-G protein between SYF and Src+ could be detected using this procedure (Fig. 5, *M*). These findings indicate that genetic deletion of Src has no significant effect on the anterograde protein transport.

DISCUSSION

We reported previously that Src activation causes the recruitment of ubiquitin ligase Cbl to the Golgi apparatus (10). Our current findings reveal that SYF cells (lacking the three kinases Src, Yes, and Fyn) have a compacted Golgi apparatus with bloated cisternae compared with their normal counterparts. This compacted morphology reverts to normal when Src is expressed exogenously in SYF cells. Src family tyrosine kinases are thus required for the maintenance of normal Golgi apparatus organization. Whether Fyn and Yes can have similar effects on the Golgi apparatus is not currently known. We found that the amount of KDEL-R in the Golgi membranes in SYF and NIH3T3 cells is decreased upon expression of an activated form of Src, SrcE378G. The effect of Src is specific for KDEL-R, because other Golgi proteins, such as the cis/medial specific mannosidase II, are not affected. Following activation

of Src, KDEL-R is found in numerous punctate structures around the Golgi apparatus, suggesting that Src modifies the kinetics of KDEL-R cycle and, hence, its steady-state distribution. To test whether Src regulates retrograde traffic, we used the *Pseudomonas* exotoxin, which binds to KDEL-R in the Golgi apparatus for transport to the ER. In the absence of Src or following its inhibition by the drug SU6656, the retrograde traffic of PE was about twice as fast. A possible interpretation of this result is that the expression of Src reduces the availability of KDEL-R to bind PE by rapidly recruiting KDEL-R upon arrival in the Golgi apparatus. Previous studies have shown that the expression of an excess of KDEL ligand had a protective effect on cells exposed to the toxin PE (21). By analogy, it is conceivable that Src induces a specific substrate to traffic more rapidly to the ER and, thus, decreases the availability of KDEL-R for binding to PE. However, the identity of the ligand that binds to KDEL-R upon Src activation is not known.

Using the viral protein VSV-GtsO45 as a marker of anterograde traffic, we could not detect any effect on its transport along the secretory pathway upon genetic deletion (Fig. 5) or by pharmacological inhibition of Src (data not shown). This suggests that Src does not play a major role in constitutive transport of secretory protein. We also tested the kinetics of anterograde traffic of Golgi enzymes from the ER upon recovery of a brefeldin A treatment and we found no difference in SYF and SYFsrc cells.[2] As Src-like kinases are not present in yeast, the Src-dependent regulation of retrograde traffic has to be specific for higher eukaryotes. How Src affects the Golgi organization and specific KDELR dynamics are the obvious challenges given the important oncogenic potential of this kinase.

REFERENCES

1. Martin, G. S. (2001) *Nat. Rev. Mol. Cell Biol.* **2,** 467–475
2. Bjorge, J. D., Jakymiw, A., and Fujita, D. J. (2000) *Oncogene* **19,** 5620–5635
3. David-Pfeuty, T., and Nouvian-Dooghe, Y. (1990) *J. Cell Biol.* **111,** 3097–3116
4. Linstedt, A. D., Vetter, M. L., Bishop, J. M., and Kelly, R. B. (1992) *J. Cell Biol.* **117,** 1077–1084
5. Foster-Barber, A., and Bishop, J. M. (1998) *Proc. Natl. Acad. Sci. U. S. A.* **95,** 4673–4677
6. Onofri, F., Giovedi, S., Kao, H. T., Valtorta, F., Borbone, L. B., De Camilli, P., Greengard, P., and Benfenati, F. (2000) *J. Biol. Chem.* **275,** 29857–29867
7. Onofri, F., Giovedi, S., Vaccaro, P., Czernik, A. J., Valtorta, F., De Camilli, P., Greengard, P., and Benfenati, F. (1997) *Proc. Natl. Acad. Sci. U. S. A.* **94,** 12168–12173
8. Barnekow, A., Jahn, R., and Schartl, M. (1990) *Oncogene* **5,** 1019–1024
9. Janz, R., and Sudhof, T. C. (1998) *J. Biol. Chem.* **273,** 2851–2857
10. Bard, F., Patel, U., Levy, J. B., Horne, W. C., Jurdic, P., and Baron, R. (2002) *Eur. J. Cell Biol.* **81,** 26–35
11. Chiu, V. K., Bivona, T., Hach, A., Sajous, J. B., Silletti, J., Wiener, H., Johnson, R. L., Cox, A. D., and Philips, M. R. (2002) *Nat. Cell Biol.* **4,** 343–350
12. Jakymiw, A., Raharjo, E., Rattner, J. B., Eystathioy, T., Chan, E. K., and Fujita, D. J. (2000) *J. Biol. Chem.* **275,** 4137–4144
13. Jamora, C., Takizawa, P. A., Zaarour, R. F., Denesvre, C., Faulkner, D. J., and Malhotra, V. (1997) *Cell* **91,** 617–626
14. Liljedahl, M., Maeda, Y., Colanzi, A., Ayala, I., Van Lint, J., and Malhotra, V. (2001) *Cell* **104,** 409–420
15. Colanzi, A., Deerinck, T. J., Ellisman, M. H., and Malhotra, V. (2000) *J. Cell Biol.* **149,** 331–339
16. Acharya, U., Mallabiabarrena, A., Acharya, J. K., and Malhotra, V. (1998) *Cell* **92,** 183–192
17. Sutterlin, C., Lin, C. Y., Feng, Y., Ferris, D. K., Erikson, R. L., and Malhotra, V. (2001) *Proc. Natl. Acad. Sci. U. S. A.* **98,** 9128–9132
18. Thomas, S. M., and Brugge, J. S. (1997) *Annu. Rev. Cell Dev. Biol.* **13,** 513–609
19. Klinghoffer, R. A., Sachsenmaier, C., Cooper, J. A., and Soriano, P. (1999) *EMBO J.* **18,** 2459–2471
20. Lewis, M. J., and Pelham, H. R. (1992) *Cell* **68,** 353–364
21. Jackson, M. E., Simpson, J. C., Girod, A., Pepperkok, R., Roberts, L. M., and Lord, J. M. (1999) *J. Cell Sci.* **112,** 467–475
22. Sandvig, K., and Van Deurs, B. (2002) *Annu. Rev. Cell Dev. Biol.* **18,** 1–24
23. Blake, R. A., Broome, M. A., Liu, X., Wu, J., Gishizky, M., Sun, L., and Courtneidge, S. A. (2000) *Mol. Cell. Biol.* **20,** 9018–9027
24. Griffiths, G., Pfeiffer, S., Simons, K., and Matlin, K. (1985) *J. Cell Biol.* **101,** 949–964

Src Regulates Golgi Structure and KDEL Receptor-dependent Retrograde Transport to the Endoplasmic Reticulum

Frédéric Bard, Laetitia Mazelin, Christine Péchoux-Longin, Vivek Malhotra and Pierre Jurdic

Access the most updated version of this article at doi: 10.1074/jbc.M302221200

Alerts:
- When this article is cited
- When a correction for this article is posted

Click here to choose from all of JBC's e-mail alerts

This article cites 24 references, 13 of which can be accessed free at
http://www.jbc.org/content/278/47/46601.full.html#ref-list-1